Multi-Aspect Angle Classification of Human Radar Signatures

C. Karabacak[a], S.Z. Gürbüz*[a,b], M.B. Guldogan[c], A.C. Gürbüz[a]
[a]TOBB Univ. of Economics and Technology, Dept. of Electrical-Electronics Eng., Ankara, Turkey;
[b]TUBITAK Space Tech. Research Institute, Image Processing Group, Ankara, Turkey;
[c]Turgut Ozal University, Dept. of Electrical-Electronics Eng., Ankara, Turkey;

ABSTRACT

The human micro-Doppler signature is a unique signature caused by the time-varying motion of each point on the human body, which can be used to discriminate humans from other targets exhibiting micro-Doppler, such as vehicles, tanks, helicopters, and even other animals. Classification of targets based on micro-Doppler generally involves joint time-frequency analysis of the radar return coupled with extraction of features that may be used to identify the target. Although many techniques have been investigated, including artificial neural networks and support vector machines, almost all suffer a drastic drop in classification performance as the aspect angle of human motion relative to the radar increases. This paper focuses on the use of radar networks to obtain multi-aspect angle data and thereby ameliorate the dependence of classification performance on aspect angle. Knowledge of human walking kinematics is exploited to generate a fuse spectrogram that incorporates estimates of model parameters obtained from each radar in the network. It is shown that the fused spectrogram better approximates the truly underlying motion of the target observed as compared with spectrograms generated from individual nodes.

Keywords: human micro-Doppler, human classification, data fusion, radar networks

1. INTRODUCTION

The micro-Doppler signature [1,2] of a target provides a basis for discriminating, classifying, and identifying targets possessing micro-motion dynamics, small-amplitude vibrations or rotation of any part of the target. The rotational motion of vehicle wheels, tank treads or helicopter blades are all examples of micro-motion dynamics that result in micro-Doppler frequency modulations in addition to the Doppler shift caused by the translational motion of the target. The time-frequency patterns that characterize a target's micro-Doppler signature can be used to identify and classify a wide-range of targets, including humans and animals. The human micro-Doppler signature is especially unique because the bi-pedal nature of human motion generates distinct patterns, differentiable from that of the quadruped motion of animals [3,4]. Moreover, the human micro-Doppler signature also reflects variations dependent upon the activity being engaged in, thereby enabling the potential to classify whether a person is walking, running, jumping, or crawling, among other potential activities.

Indeed a variety of classification algorithms, each exploiting a differing feature set, have been proposed for the purposes of human classification, including artificial neural networks [5], support vector machines [6], principal component analysis [7,8], linear discriminant analysis [7], statistics [9], distance measures [10], k-means [11], Bayesian probability theory [12], and information theory [13,14]. However, all of these techniques typically only perform well if the target directly moves towards the radar. As the aspect angle between the target and radar increases, classification continuously decreases, reaching its poorest level when the target tangentially by-passes the radar at an aspect angle of 90 degrees. It has been reported that in this case classification performance can drop to as low as 40% [15]. This is because the radial velocity measured by the radar decreases as the aspect angle increases, leading to spectrograms with small Doppler frequency modulations from which it is difficult to obtain accurate feature estimates.

One way to compensate for the degradation in classification performance due to aspect angle is to employ a multistatic radar network, which is capable of obtaining multi-aspect angle data. There has been little work on the use of multistatic radar for the detection and classification of human targets. However, notable results have been achieved by G.E. Smith and C.J. Baker of the University College London, UK, who have examined the multistatic human signature with both simulations and experimental tests. Simulated human micro-Doppler signatures were obtained by modeling

*szgurbuz@etu.edu.tr, sevgi.gurbuz@tubitak.gov.tr; phone +90-312-292-4072; fax +90-312-292-4180

the person as being comprised only of three parts: the torso and two legs. Although a more simplistic model than the Boulic model [16] that is more widely used, results show that simulated human spectrograms visually match those obtained by measurements from a three-node 2.4 GHz radar network, NetRAD [17]. Moreover, by computing the correlation of data received at each node, Smith and Baker argued that the multiple angle observations offer extra information in comparison to the monostatic case, which can be exploited for automatic target recognition (ATR). A multi-perspective, template based classifier was proposed [18] using a combined feature vector that incorporates data from all possible bistatic paths within the network. Three classes - wheeled vehicle, bicycle and personnel - were successfully discriminated with an average probability of correct classification of 97%; however, this probability dropped to %24 for generalized targets within a class.

This work examines in detail the problem of classifying human targets and their activities with a radar network. The multistatic human micro-Doppler signature is computed from simulated radar data generated from two different types of human animations. One, the Boulic kinematic model is used for walking; and two, video motion capture data is used animate a wide range of potential human motions, including walking. The multistatic micro-Doppler signatures obtained from these two animation techniques are then compared. Next, the problem of data fusion within a radar network is discussed. Ultimately, the observations of all nodes within the network are of the same phenomenon: human movement. However, since the observation angle of each radar differs, the accuracy of features extracted differs from node to node. The question of how to exploit these feature estimates is explored in light of determining the key parameters that define the underlying motion. These estimates are then used to generate a *single fused spectrogram* from the multistatic radar data. It is shown that the fused spectrogram offers a clearer representation of fusion motion that is not drastically degraded by aspect angle variations, and can be exploited in human classification problems.

2. MULTISTATIC HUMAN MICRO-DOPPLER

2.1 Multistatic Radar Response from Pointwise Decomposition of Human Target

For a point target, the received signal of a pulsed Doppler radar transmitting a chirp signal at a fixed pulse repetition interval (PRI) is a time-delayed and frequency-shifted version of the transmitted signal. Work by Van Dorp [19] and Geisheimer [20] has shown that the overall response from a human target can be represented as the superposition of responses from each point on the human body. Suppose the human body was decomposed into K point targets; then, the total receive signal may be written as

$$s_h(n,t) = \sum_{i=1}^{K} a_{t,i}\, rect\left(\frac{\hat{t} - t_{d,i}}{\tau}\right) e^{j[-2\pi f_c t_{d,i} + \pi\gamma(\hat{t} - t_{d,i})^2]}, \tag{1}$$

where the time t is defined as $t = T(n-1) + \hat{t}$ in terms of the pulse repetition interval (PRI), T, the pulse number, n, and the time relative to the start of each PRI, $\hat{t}$; a_t is the amplitude as given by the radar range equation; τ is the pulse width; c is the speed of light; γ is the chirp slope; f_c is the transmitted center frequency; and t_d is the round-trip time delay between antenna and target, defined in terms of the target range, R, as $t_d = 2R/c$. Moreover, $a_{t,i}$ and $t_{d,i}$ are the amplitude and time delay of the return of each body part.

The amplitude $a_{t,i}$, is computed from the radar range equation as

$$a_{t,i} = \frac{G\lambda\sqrt{P_t\sigma_i}\,\sigma_n}{(4\pi)^{1.5} R_i^2 \sqrt{L_s}\sqrt{L_a}\sqrt{T_{sys}}}, \tag{2}$$

where G is the antenna gain, λ is the wavelength, L_a represents atmospheric losses, L_s system losses, T_{sys} system temperature, P_t transmitter power, σ_n noise standard deviation, and σ_i the RCS of the i^{th} body part. Not all of these parameters remain constant. For example, the gain can vary according to angle incidence depending on the antenna beam

pattern, and the atmospheric losses vary with range. However, for simplicity, all parameters are modeled as constants. The RCS of each body part is approximated by that either a sphere, cylinder or ellipsoid, depending on which most closely matches. So, a sphere is used to approximate the head, while either a cylinder or ellipsoid is used for the torso and limbs.

If the constant parameters are collected as a single parameter, A, then the amplitude factor for each body part may be expressed more simply as

$$a_{t,i} = \frac{A_i}{R_i^2}. \tag{3}$$

The received return from the human target, stored as a slow-time, fast-time data matrix, is then pulse compressed so that the peak occurs at the range bin in which the target is present. Taking a slice across slow-time at the range bin of the peak output,

$$x_p[n] = \sum_{i=1}^{K} A_i \tau e^{-j\frac{4\pi f_c}{c} R_{d,i}}, \tag{4}$$

where $R_{d,i}$ is the range from the antenna to the center of each body part.

In the multistatic case, the radar network forms N_{TX} x N_{RX} bistatic paths. N_{TX} is the number of transmit nodes and N_{RX} is the number of receive nodes. Thus, the range term $R_{d,i}$ is now not the round-trip range, but the bistatic range – the sum of the range between each node and the target. Define $\mathbf{r_{tn}}$ as the target range when the n^{th} pulse is transmitted. The target moves along a path, assumed in this work to be linear, which is defined by the vector **h**. After the transmission of n pulses, the target position may be expressed as the sum of a translational and micro-motion component, **μ**, caused by body part oscillations:

$$\begin{aligned} \mathbf{r_{tn}} &= \mathbf{r_{r1}} + \mathbf{h} + \boldsymbol{\mu} \\ \mathbf{r_{rn}} &= \mathbf{r_{r1}} + \mathbf{h} + \boldsymbol{\mu} \end{aligned} \tag{4}$$

Thus, the expected multi-static human response is

$$x_p[n] = \sum_{i=1}^{12} A_i \tau e^{-j\frac{4\pi f_c}{c}|\mathbf{r_{tn}}+\mathbf{r_{rn}}|_i}. \tag{5}$$

The time-varying position of each body part, as represented by **h+μ**, can be computed from kinematic models, such as the Boulic model, or from video motion capture data. Each method is discussed in turn.

2.2 Boulic Kinematic Model for Walking

The Boulic kinematic model is based on experimental biomechanical data, and is valid only for walking. In the model, the human body is represented as a stick figure, with lines linking the main joints of the human body. The change of the angles between various links as well as the translation of the origin OS, situated at the base of the spine, is provided over the duration of one cycle (two steps). Thereafter, the walking motion is assumed to repeat identically. Mathematically, the Boulic model expresses with equations the time-varying position of certain critical points, such as OS, while the variation of joint angles with time are given in terms of graphical charts. Thus, the Boulic model is not a closed-form model; however, the information provided, when used in conjunction with human body dimensions, can be used to reconstruct the time-varying position of 17 points that are critical to identifying human gait.

All equations and charts revolve around a single key parameter: the relative velocity (RV), which is defined as the ratio of velocity (v) to the height of thigh (HT):

$$RV = V/HT \tag{6}$$

Based on the relative velocity, key gait parameters such as the relative length of the gait cycle (RLC) and duration of the cycle (DC) can be calculated as

$$RLC = 1.346 \times \sqrt{RV} \tag{7}$$

$$DC = RLC / RV \tag{8}$$

These three equations are important because they can be used to derive a formula showing that the relative velocity is dependent on cycle duration, as given in (9), and, more importantly, if the cycle duration and velocity of the person are known, the thigh height can be calculated easily as follows:

$$RV = \left(1.346/DC\right)^2 \tag{9}$$

$$HT = V \times \left(DC/1.346\right)^2 \tag{10}$$

As will be seen in Section 3, (10) will be used extensively as a means of extracting information about the physical features of the target being observed.

2.3 Animation with Video Motion Capture Data

A key limitation of the Boulic model is that it is only applicable to walking, whereas the range of potential human movements is significantly broader. Moreover, the spectrogram generated by the Boulic model is quite "clean" in comparison that derived from measured radar data, yielding easier obtainable, more accurate feature estimates and thus greater classification performance. A more realistic human spectrogram for a wider range of activities can be obtained by instead computing the time-varying ranges from motion capture data of human movement.

The Carnegie Mellon University (CMU) Motion Research Laboratory has developed a library of human motion capture data [21], which it distributes free of charge to researchers worldwide. The CMU database contains data of many different people engaged in a variety of motions, including walking, running, climbing, crawling, jumping, different sports, and composite activities, such as running – stopping – and running again. The data was collected with the aid of 41 sensors placed on the human body and was recorded by 12 infrared cameras at a frequency of 120 Hz. The database contains a total of 2605 different motion records belonging to 112 different subjects.

The main difference between the human spectrograms generated from motion capture data and those generated using the Boulic model is that the curves in the spectrogram generated from CMU data are not as sharp or well defined as that computed from the Boulic model. Indeed, it has been shown that spectrograms generated from motion capture data much more closely match with measured spectrograms than those that generate from models [22, 23]. Thus, in this work results are presented for both model generated and motion capture generated data.

3. TIME-FREQUENCY FUSION OF HUMAN MICRO-DOPPLER

In general, a network comprised of M radars contains M monostatic paths and $\binom{M}{2} = \frac{M!}{2(M-2)!}$ bistatic paths. From each path, a different micro-Doppler signature yielding estimates for N features may be obtained. Thus, the total number of feature estimates is given by $\left[M + \frac{M!}{2(M-2)!}\right] \times N$. One possible scheme for exploiting this data is to treat each estimate equally and form a single combined feature vector upon which any classification algorithm of choice may be applied. However, such an even-handed approach fails to taken into account that in fact the feature estimates obtained are *related*: each set of N estimates offer a description of the *same underlying phenomenon*, the movement of a single human target.

From gait analysis, we know that human motion possesses *structure*, resulting from the geometric constraints imposed by the human body. The features we extract from the spectrogram are in fact just a pale reflection of the entire time-frequency signature that fully defines this structure. Now, suppose for a moment that we had a mathematical

description of the underlying structure – we simply didn't know the specific model parameters values corresponding to the movement being observed. Then, by estimating these model parameters, we would be able to not just determine the activity being conducted, but also we would be able to *reconstruct* the underlying motion being observed by all nodes within the network. For the case of walking, just such a model already exists: the Boulic kinematic model. Given the velocity and height of thigh of a human, using the Boulic model, the entire human micro-Doppler signature can be reconstructed.

Thus, in this work, rather than using network observations independently, we propose using the observations with the realization that the same event is being observed. Rather than extract multitudes of features whose degree of contribution to the classification problem is unknown, all we really need to classify human walking is just two parameters: V and HT. This approach will also enable us to make our classification algorithms less sensitive on aspect angle. Now, the feature estimates will be obtained not based on the individual measurements of each radar, but from the joint estimates of all nodes within the network, with the goal of generating a *single fused human micro-Doppler signature*, as generated by the Boulic model.

3.1 Estimating Model of Underlying Motion

The Boulic model parameters, velocity and height of thigh, are extracted from the micro-Doppler measurements of each node as follows. The torso Doppler frequency (f_D) can be used to obtain the radial velocity (V_{rad}) of the target as in (11), where f_C is the frequency of the electromagnetic wave and c is the velocity of the light:

$$f_D = \left(2 \cdot f_C / c\right) \cdot \left|V_{rad}\right|. \tag{11}$$

The velocity of the target can be calculated by using V_{rad} in terms of the aspect angle (α) between target and radar, relative to the direct line of sight:

$$\left|V_{rad}\right| = \left|V\right| \cdot \cos\left(\alpha\right) \tag{12}$$

As an example for this paper, we used a single-input multiple-output (SIMO) radar network consisting of one transmitter and three receivers. All antennas are placed co-linearly, with the target located at an initial distance of 1000 m from the transmitter, as shown in Figure 1. Simulations are conducted with a total dwell time of 4 seconds, and for a range of aspect angles between 0° and 90°. The target velocity was set at 1 m/s with body part dimensions as listed in Table 1. Simulated data was then generated using both the Boulic model and the CMU motion capture database to generate the micro-Doppler signature of a human walking as measured by the radar network.

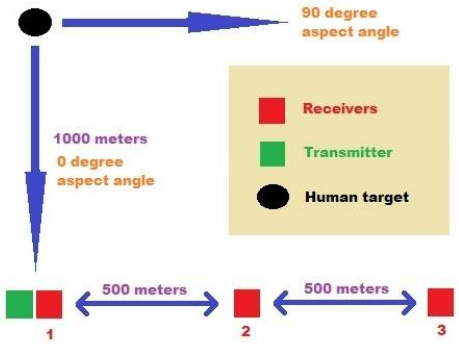

Figure 1. Radar Network Topology

Body Part	Length (m)	Shape
Head	0.41	Sphere
Torso	0.8	Ellipsoid
Upper Leg	0.55	Ellipsoid
Lower Leg	0.49	Ellipsoid
Upper Arm	0.395	Ellipsoid
Lower Arm	0.305	Ellipsoid
Feet	0.285	Ellipsoid

Table 1. Human Model Parameters

In the context of the radar network described above, we assume that the total distance traveled (about 4 m) is small relative to the distance to the radar (1000 m) so that the aspect angles do not change significantly over the duration of the simulation. Thus, the aspect angle of the target relative to each radar in the network can be computed from Figure 2 by

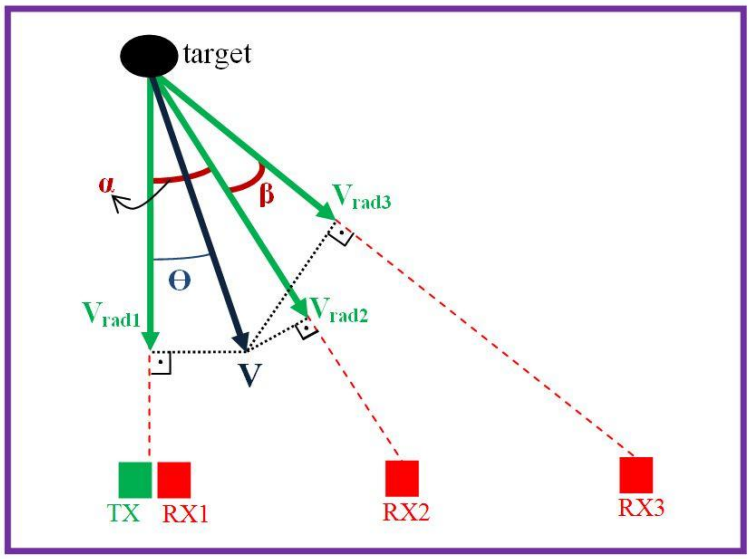

Figure 2. Key angles required for target velocity estimation.

calculating the projection of the target motion vector onto the line of direct path between the target and each radar. For the particular network topology given in Figure 1, this results in $\alpha \approx 26.57^{\circ}$ and $\beta = 45^{\circ}$. We thus obtain three equations, one for each required radial velocity:

$$\begin{aligned} |V_{rad1}| &= |V| \cdot \cos(\theta) \\ |V_{rad2}| &= |V| \cdot \cos(\alpha - \theta) \\ |V_{rad3}| &= |V| \cdot \cos(\alpha + \beta - \theta) \end{aligned} \tag{13}$$

This is a over-determined, nonlinear system because with two unknown parameters (V and Θ) and three equations. Since exact solution of this system is not possible for every condition, the Levenberg-Maquardt-Fletcher [24] algorithm is used to find a single solution that minimizes the nonlinear least squares error. In this way, estimates for the target velocity V and angle of motion, θ, are obtained.

Recall that from (10), the height of thigh may be computed given knowledge of the target velocity and duration of cycle (DC). The duration of cycle is equal to the period of limb motion, which are extracted from the spectrograms measured at each node and then averaged to yield a single estimate:

$$DC_{est} = \left(DC_{rec1} + DC_{rec2} + DC_{rec3}\right)/3 \tag{14}$$

Correct estimation of HT is critical because it provides information about the length of human body parts. In [25], body parts dimensions for the statistically smallest and largest male and female are given. As human height is Gaussian distributed, we assume that body part sizes are also Gaussian distributed. Given an estimate of HT, this may then be used to scale each body part size to be consistent with our observations. These dimensions, along with the estimates of V and HT, are given as inputs to the Boulic model, which can then regenerate the observed human micro-Doppler as if the target were walking directly towards a monostatic radar system - the *fused spectrogram*.

A similar process is applied on data generated from the CMU motion capture data. Estimates are obtained with the same procedure described above, and the fused spectrogram is generated by the Boulic model based on the model parameter estimates obtained.

3.2 Fused Spectrogram

In this section, fusion results for different target motion aspect angles with estimates derived from both Boulic model and CMU motion capture generated data is given. First consider human micro-Doppler signatures generated from the Boulic model. When the radar-target aspect angle is 45°, the individual spectrograms obtained by Receivers 1, 2, and 3 are shown in Figure 3. Notice that at all angles the micro-Doppler characteristics of the torso, arms, and legs are clearly visible. In this case, the 45° aspect angle does not severely degrade the human signatures. As would be expected, the fused spectrogram generated based on model parameter estimates is of similar quality, as shown in Figure 4.

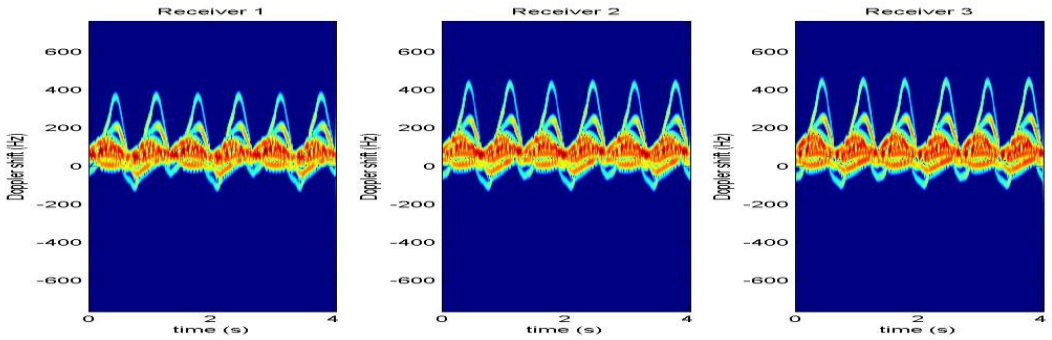

Figure 3. Simulation results on data generated with the Boulic Model when the aspect angle is 45 degrees.

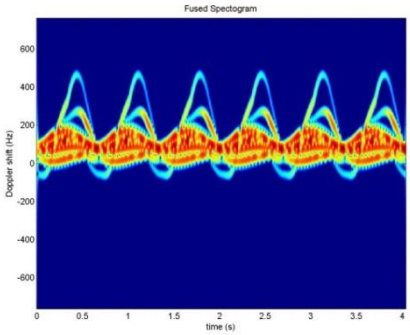

Figure 4. Fused spectrogram generated from Figure 3 measurements.

However, when the aspect angle increases to 90°, the micro-Doppler signatures obtained at the three receivers are much degraded in comparison to those obtained when the aspect angle was 45°, as shown in Figure 5. The spectrograms measured by Receivers 1 and 2 exhibit only the torso micro-Doppler, with Receiver 3 data barely reflecting the micro-Doppler component of the legs. Compare these spectrograms, however, to the fused spectrogram obtained based on model parameter estimates (Figure 6). In the fused spectrograms, the true micro-Doppler of the underlying human motion is now clear.

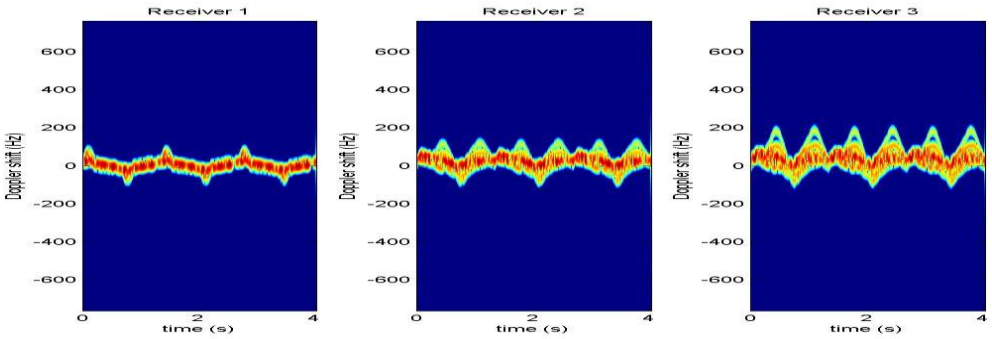

Figure 5. Simulation results on data generated with the Boulic Model when the aspect angle is 90 degrees.

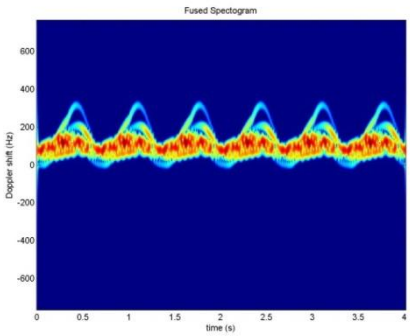

Figure 6. Fused spectrogram generated from Figure 5 measurements.

Now consider the same experiments repeated for data generated with the more realistic motion capture data. The individual spectrograms measured by the network for an aspect angle of 30° are shown in Figure 7, with the resulting fused spectrogram shown in Figure 8. The quality of model parameter estimates decreases to the noisier nature of the motion capture data, however, still a much clearer fused spectrogram is obtained. The benefit of fusion is made even more clear when the aspect angle increases to 75°, as shown in Figures 9 and 10. In this case the individual spectrograms exhibit no visually observable micro-Doppler, beyond that of torso motion, but with fusion a closer approximation to the true underlying human signature is obtained.

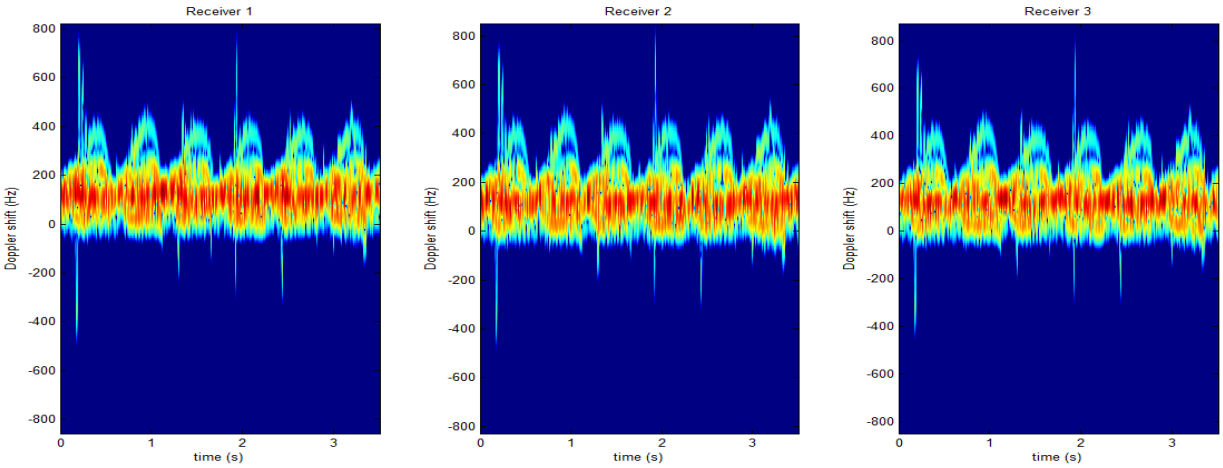

Figure 7. Simulation results on data generated with the motion capture when the aspect angle is 30 degrees.

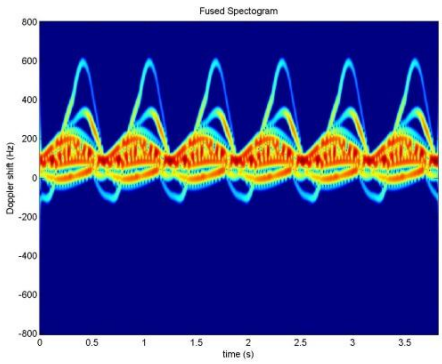

Figure 8. Fused spectrogram generated from Figure 7 measurements.

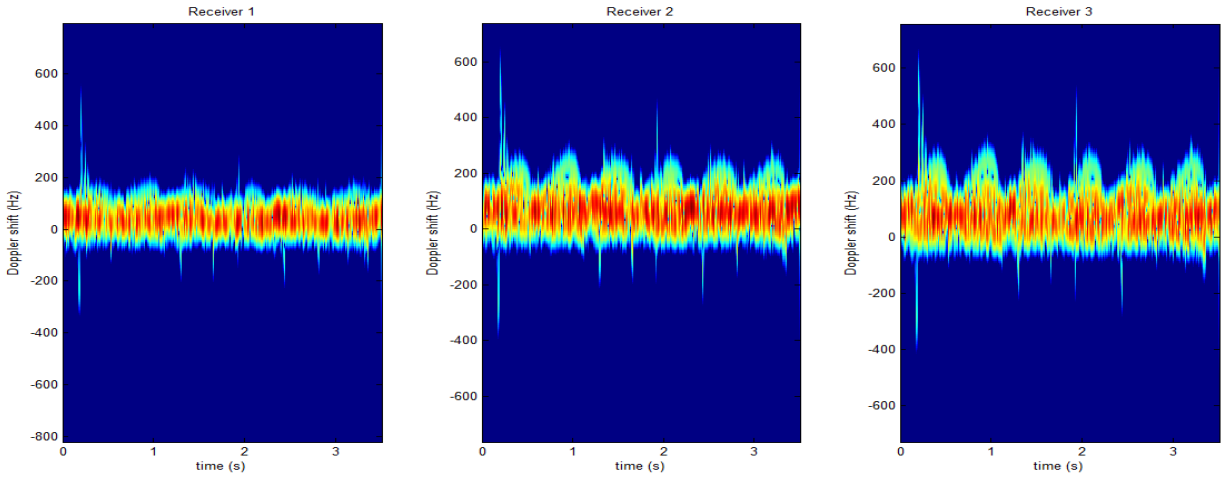

Figure 9. Simulation results on data generated with the motion capture when the aspect angle is 75 degrees.

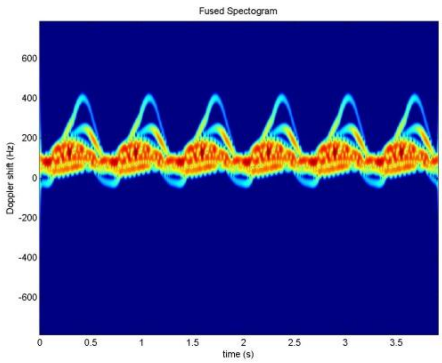

Figure 10. Fused spectrogram generated from Figure 9 measurements.

4. CONCLUSIONS AND FUTURE WORK

In this paper, multistatic radar data is exploited to estimate the parameters of human kinematic model, which in turn is used to generate a single fused spectrogram representative of the true human motion observed by all nodes within the radar network. It is shown that the fused spectrogram offers a clearer picture of human micro-Doppler than the individual spectrograms obtained by each radar independently, especially in the case when the radar-target aspect angle is high, resulting in minute micro-Doppler modulations. In future work, the fused spectrograms will be used in the classification of human activities with a radar network. With the development of kinematic models for other human activities, these results can also be generalized to a wider range of human motions.

ACKNOWLEDGEMENTS

This work was supported in part by EU FP7 Project No. PIRG-GA-2010-268276 (COGSENSE).

REFERENCES

[1] Chen, V.C., Li, F., Ho, S.-S., and Wechsler, H., "Micro-doppler effect in radar: phenomenon, model, and simulation study," IEEE Trans. Aerospace and Electronics Systems, Vol. 42, No. 1, 2006, pp. 2-21.

[2] Chen, V.C., [The Micro-Doppler Effect in Radar], Artech House, 2010.

[3] Tahmoush, D., and Silvious, J., "Remote detection of humans and animals," Proc. IEEE AIPR Workshop, 2009.

[4] Otero, M., "Application of a continuous wave radar for human gait recognition", Proc. of SPIE, Vol. 5809, pp. 538-548, 2005.

[5] Kim, Y., and Ling, H., "Human activity classification based on micro-Doppler signatures using an artificial neural network," Proc. Int. Symposium of the Antennas and Propagation Society, 2008.

[6] Kim, Y., and Ling, H., "Human activity classification based on micro-Doppler signatures using a support vector machine," IEEE Trans. Geoscience and Remote Sensing, Vol. 47, No. 5, 2009, pp. 1328-1337.

[7] Li, J., Phung, S.L., Tivive, F.H.C., and Bouzerdoum, A., "Automatic classification of human motions using Doppler radar," Proc. IEEE World Congress on Comp. Intelligence (WCCI), Brisbane, June 10-15, 2012.

[8] Mobasseri, B.G., and Amin, M.G., "A time-frequency classifier for human gait recognition." Proc. SPIE 7306, May 05, 2009.

[9] Yang, Y., Lei, J., Zhang, W., and Lu, C., "Target classification and pattern recognition using micro-doppler radar signatures," 7th Annual Conf. on Software Engineering, Artificial Intelligence, Networking, and Parallel/Distributed Computing (SNPD), pp.213-217, 19-20 June 2006.

[10] Lyonnet, B., Ioana, C., and Amin, M., "Human gait classification using Micro Doppler time-frequency signal representations," Proc. IEEE Radar Conference, 2010.

[11] Garreau, G., Andreou, C.M., Andreou, A., and Georgiou, J., "Gait-based person and gender recognition using micro-doppler signatures," Proc. IEEE Biomedical Circuits and Systems Conference (BioCAS), 2011.

[12] Nanzer, J.A., and Rogers, R.L., "Bayesian classification of humans and vehicles using micro-doppler signals from a scanning-beam radar," IEEE *Microwave and Wireless Components Letters*, Vol. 19, No. 5, pp. 338-340, May 2009.

[13] Imer, J.W., Bing, K.F., Sharma, A.C., and Greneker, E.F., "Detecting concussion impairment with radar using gait analysis techniques," IEEE Radar Conference, pp.222-225, 23-27 May 2011.

[14] Tekeli, B., Gurbuz, S.Z., Yuksel, M., Gurbuz, A.C., and Guldogan, M.B., "Classification of human micro-doppler in a radar network," IEEE Radar Conference, 29 April-3 May, 2013.

[15] Tahmoush, D., and Silvious, J., "Radar micro-Doppler for long range front-fiew gait recognition," Proc. IEEE 3rd Int. Conf. on Biometrics: Theory, Applications, Systems, 2009.

[16] Boulic, R., Thalmann, M.N., and Thalmann, D., "A global walking model with real-time kinematic personification," Visual Computing, Vol. 6, pp. 344-358, 1990.

[17] Smith, G.E., Woodbridge, K., Baker, C.J., and Griffiths, H., "Multistatic micro-doppler radar signatures of personnel targets," IET Signal Processing, Special Issue on Time-Frequency Approach to Radar Detection, Imaging, and Classification, Vol. 4, Iss. 3, pp. 224-233, 2010.

[18] Smith, G.E., Woodbridge, K., and Baker, C.J., "Multiperspective micro-doppler signature classification," Proc. IET Int. Conf. on Radar Systems, Edinburgh, October 2007.

[19] Van Dorp, P., and Groen, F.C.A., "Human walking estimation with radar," IEE Proc. on Radar, Sonar, and Navigation, Vol. 155, No. 5, pp. 356-365, 2003.

[20] Geisheimer, J.L., Greneker, E.F., and Marshall, W.S., "A high resolution doppler model of human gait," Proc. of SPIE, Vol. 4744, 2002.

[21] The Motion Research Laboratory, Carnegie Mellon University (CMU), http://mocap.cs.cmu.edu

[22] Karabacak, C., Gurbuz, S.Z., and Gurbuz, A.C., "Radar simulation of human micro-Doppler signature from video motion capture data," IEEE Signal Processing and Communications Applications Conference (SIU), Girne, Turkish Republic of Northern Cyprus, April 2013.

[23] Ram, S.S., and Ling, H., "Simulation of human micro-Dopplers using computer animation data," IEEE Radar Conference, 2008.

[24] http://www.mathworks.com/matlabcentral/fileexchange/16063-lmfsolvem-levenberg-

[25] S.Z. Gurbuz, "Human Detection with Radar: Dismount Detection" in [Principles of Modern Radar: Advanced Techniques], Sci Tech Publishing, 2012.